

Accepted Manuscript

Domain nucleation behavior in ferroelectric films with thin and ultrathin top electrodes versus insulating top layers

L.J. McGilly, L. Feigl, N. Setter

PII: S0040-6090(17)30322-X
DOI: doi: [10.1016/j.tsf.2017.04.046](https://doi.org/10.1016/j.tsf.2017.04.046)
Reference: TSF 35954
To appear in: *Thin Solid Films*
Received date: 18 July 2016
Revised date: 10 April 2017
Accepted date: 29 April 2017



Please cite this article as: L.J. McGilly, L. Feigl, N. Setter , Domain nucleation behavior in ferroelectric films with thin and ultrathin top electrodes versus insulating top layers, *Thin Solid Films* (2017), doi: [10.1016/j.tsf.2017.04.046](https://doi.org/10.1016/j.tsf.2017.04.046)

This is a PDF file of an unedited manuscript that has been accepted for publication. As a service to our customers we are providing this early version of the manuscript. The manuscript will undergo copyediting, typesetting, and review of the resulting proof before it is published in its final form. Please note that during the production process errors may be discovered which could affect the content, and all legal disclaimers that apply to the journal pertain.

Domain nucleation behavior in ferroelectric films with thin and ultrathin top electrodes versus insulating top layers

L. J. McGilly^{a*}, L. Feigl^{a,b} and N. Setter^{a,c}

^aCeramics Laboratory, EPFL - Swiss Federal Institute of Technology, Lausanne, CH-1015 Switzerland

^bInstitute for Photon Science and Synchrotron Radiation, KIT - Karlsruhe Institute of Technology, Hermann-von-Helmholtz-Platz 1, D-76344 Eggenstein-Leopoldshafen, Germany

^cDepartment of Materials Science and Engineering, Tel-Aviv University, Ramat Aviv 69978, Israel

*Corresponding author at: Ceramics Laboratory, EPFL - Swiss Federal Institute of Technology, Lausanne, CH-1015 Switzerland. Email: leo.mcgilley@epfl.ch

The effect of varying the thickness of Pt top electrodes made by the electron beam induced deposition technique on the domain nucleation characteristics of $\text{Pb}(\text{Zr,Ti})\text{O}_3$ films has been investigated by piezoresponse force microscopy. The advantage of this experimental setup is that the nucleation position can be precisely controlled allowing comparison between two capacitor structures with different top electrode thicknesses and negating the role of defect-induced polarization switching scenarios. In the ultrathin limit (<5 nm), the coercive biases of polarization switching change substantially relative to thicker electrodes, from -4.6 to -2.6 V and from +3.5 to 5.5 V respectively, which we link to a work function size effect. The evolution of the piezoresponse and coercive biases as a function of hysteresis loop cycling is presented and contrasted with that obtained on the bare film surface with no top electrode. To provide a counterpoint to the observed effects with top electrodes, we have demonstrated the variation in switching due to a top silicon oxide insulating layer. This work has revealed a method which could be used to control nucleation bias in ferroelectric thin film systems.

Keywords: nanotechnology, ferroelectric, domain walls, thin films, scanning probe microscopy, hysteresis, polarization switching, piezoresponse force microscopy

1. Introduction

Polarization switching is a key feature of ferroelectric materials and has been intensively studied in single crystals and ceramics since the discovery of ferroelectricity. Polarization reversal occurs when the local electric field is sufficient to create a nucleus which then grows under continued applied fields to complete ferroelectric switching through domain wall motion [1]. In this widely accepted model, capacitors with metal electrodes have nucleation points which are uncontrolled and occur stochastically at defects [2]. A common method uses displacement currents that result from the necessary compensation of bound polarization charge upon polar vector reorientation to give information on switching [3]. However this gives a global picture of switching in the ferroelectric capacitor without spatial information. Only recently has it become possible to reproducibly determine the domain nucleation points in thin films [4]-[9][8]. Using this ability we can now directly compare the nucleation and switching behavior of a range of top electrodes and insulating layers.

Using high resistivity electrodes made via electron beam induced deposition (EBID) of Pt [9]-[12] we can control the nucleation point of the domains through positioning of a piezoresponse force microscopy (PFM) tip during voltage pulsing [7]. This allows us to study the effect of changing the electrode thickness on the nucleation of domains. Recently we demonstrated how the top electrode thickness determines the velocity with which a domain wall will propagate via a resistivity size effect [13]. In this study we show that the coercive bias depends on the thickness of the electrode used and this dependence is sensitive in the limit of ultrathin electrodes. Furthermore we contrast this behavior with that of an insulating silicon oxide spacer layer also deposited by EBID.

2. Experimental details

2.1 Electrode fabrication by EBID

EBID electrodes with an area of $1 \times 1 \mu\text{m}^2$ with thicknesses from $2 \pm 1 \text{ nm}$ up to $51 \pm 1 \text{ nm}$ were deposited on top of a $70 \text{ nm Pb}(\text{Zr}_{0.1}\text{Ti}_{0.9})\text{O}_3$ [PZT] (001) oriented film (Fig. 1a). The lower electrode in this case was 44 nm SrRuO_3 [SRO] deposited on a SrTiO_3 substrate. Pulsed laser deposition details can be found elsewhere [7]. In the as-grown state, the PZT film had uniform out-of-plane oriented polarization pointing towards the free surface *i.e.* ‘up’. EBID Pt electrodes were deposited with a $(\text{CH}_3)_3\text{CH}_3\text{C}_5\text{H}_4\text{Pt}$ precursor, a 30 kV , 1.6 nA electron beam with a pixel dwell time of 1.4 ms , a beam overlap of 60% and a base pressure of $<4 \times 10^{-6} \text{ mbar}$. The number of passes over the pattern determined the electrode thickness. The silicon oxide deposition was performed with a TEOS $[\text{Si}(\text{OCH}_2\text{CH}_3)_4]$ precursor and 5 passes of the electron beam over the pattern area. Pixel dwell time was changed from $20 \mu\text{s}$ to 1 ms to vary the thickness. Previous studies indicate that EBID Pt and silicon oxide have a large proportion of co-deposited carbon in some cases reaching $\sim 80 \text{ at\%}$ [9][11][14].

2.2 PFM and hysteresis loop measurement

An Asylum Research Cypher atomic force microscope with ASYELEC-01 Ti-Ir coated silicon probes of force constant in the range $1\text{-}3 \text{ Nm}^{-1}$ was used for PFM in the dual ac resonance tracking mode [15]. To produce hysteresis loops, piezoresponse amplitude and phase were acquired during application of a ‘chopped’ triangular waveform composed of dc bias ‘on’ and ‘off’ states with a superimposed high frequency ac probing voltage [16]. Each loop took 5 seconds to acquire. Each ‘on’ state lasted 10 ms followed by an intermediate ‘off’ state of equal duration which was in turn followed by another ‘on’ state with an incremental bias change of $\pm 0.128 \text{ V}$.

3. Results and discussion

3.1 EBID Pt top electrodes versus tip on surface case

A series of 100 hysteresis loops were acquired on each electrode as shown in Fig. 1a and on one spot on the bare film surface adjacent to the electrodes. The PFM images corresponding to an area of the bare film surface are shown in Fig. 1b and c. The lack of visible features shows the extreme

uniformity of the polarization indicating an excellent test bed for switching due to the absence of domains or large inhomogeneities. A large amount of information is obtainable from hysteresis loops in ferroelectrics [17]. An example of the loops obtained is shown in Fig. 1d where it is clear that switching is sharp, leading to rectangular hysteresis. Although the loop shape is similar for all electroded areas there is a vast difference in both the measured positive and negative coercive biases and positive and negative piezoresponse amplitudes. For such rectangular hysteresis the nucleation bias (the applied bias at which the piezoresponse changes due to formation of a nucleus) and the coercive bias (point at which piezoresponse is zero) are the same; therefore observation of coercive bias also gives the nucleation behavior. For the set of electrodes in Fig. 1a the positive and negative piezoresponses as a function of electrode thickness can be seen in Fig. 1e and the coercive biases in Fig. 1f. As could be expected, the piezoresponse decreases indicating the damping effect of the electromechanical oscillations of the ferroelectric due to increasing electrode thickness [18]. The dependency of the coercive biases (and thus nucleation) is somewhat unexpected.

As can be seen in Fig. 1f, there is a general increase in magnitude of the positive coercive bias with increasing electrode thickness while for the negative one it is more complex; switching is most difficult at an electrode thickness of 4.0 ± 0.1 nm and then eases as the electrode thickness increases. This leads to a change in polarity of the imprint. In order to confirm the trend we reproduced these experimental results several times on different days with different tips and obtained the same behavior (Fig. 1g).

Coercive bias and imprint can depend on many factors: asymmetric electrodes [19][20], interface quality [21] and depolarizing fields [22][23] certainly all lead to a built-in field that can either help or hinder polarization reversal depending on whether switching is with positive (up-to-down polarization reversal) or negative (down-to-up) bias. In the as-grown state the polarization is uniformly aligned out-of-plane up indicating a built-in field, E_i , perhaps due to a defect gradient related to growth conditions [24][25]. Furthermore we assume it does not change as the electrode thickness is changed.

We therefore designate an electric field, E_1 , that varies with changes in top electrode thickness and is aligned opposite to the native built-in field E_i such that in a simple approximation $E_{tot} = E_i - E_1$. For electrodes >20 nm E_1 varies little and is assumed to be small as the imprint is of the same polarity as the native state *i.e.* $E_{tot} > 0$. At thicknesses of ~ 5 nm imprint is zero so $E_1 = E_i$ and $E_{tot} = 0$. As E_1 continues to increase in magnitude for decreasing thicknesses in the range <5 nm $|E_1| > |E_i|$ and so $E_{tot} < 0$ as confirmed with negative imprint observed in this region.

We will now consider the possible origins of this electrode-thickness-dependent electric field. A clear candidate is a change in the depolarizing field due to changes in screening conditions at the top interface especially considering the large resistivity size effect in EBID Pt [13] and therefore a corresponding change in available screening charge carriers. However we can quickly exclude this as a major effect. The depolarizing field by definition is aligned against the initial polar state and as such should favour switching [22][26] in both senses. However as the depolarizing field decreases due to increasing electrode thickness (more available screening charges), we would expect switching to be harder in both senses but this is only true for up-down switching as evidenced by the positive coercive bias behavior. This model does not seem consistent with an increased ease of switching for down-up states (lower negative coercive bias magnitudes).

As we have asymmetric electrodes, we assume an internal field due to different work functions. We tentatively suggest a work function size effect for the EBID Pt top electrodes. To be consistent with the measured data, wherein E_1 should increase with decreasing electrode thickness, would necessitate an increasing work function with decreasing thickness. While work function size effects are typically only observed for a few monolayers to a few nanometres [27]-[29], we also note that EBID is mainly composed of Pt nanocrystallites of diameter 1-4 nm in a carbon matrix [30]. It may not be unreasonable to expect work function size effects when the film thickness is on the order of the crystallite size. Furthermore a Pt/carbon compositional gradient with thickness could perhaps allow

for large effective work function variations as amorphous carbon (which also shows size effects [31][32]) has a work function of ~ 5 eV and polycrystalline Pt of ~ 5.7 eV [33] compared to that of SRO ~ 4.6 - 4.9 eV [34].

However a conflict arises in that switching properties are reported to be independent of the electrode work function [35]-[37] while others show the opposite [19][20]. For these contrary studies the films under investigation were relatively thick >100 nm so we could expect work function differences to play a more significant role for sub-100 nm films studied here. As presented above, evidence exists for both work function size effects and for the effect of work function on hysteresis. For these reasons we therefore still maintain a work function size effect as one possible explanation of the electrode-thickness-dependent electric field, E_1 while also acknowledging that there could be multiple origins and/or contributions. Further study is required.

Next we analyse the evolution of the switching properties as a function of switching cycles (Fig. 2). There is a rapid change in both the positive and negative coercive biases for the tip-film case after around 30 switching loops (Fig. 2a). We attribute this change in the ease of switching to the growth of a small ‘dot’ (structural defect) observed at that location probably indicating an electrochemical effect [38] related to the high current density between the tip and sample surface and the presence of surface adsorbates or due to charge-injection-induced damage to the film itself. We can contrast this behavior with that of the 4 nm electrode (Fig. 2b) where the changes are more erratic with large, short-term variations however there is a general decrease in magnitude of the coercive biases. For the 11 nm electrode we see a strikingly different behavior; very stable coercive biases that hardly change over the 100 hysteresis loop range of the experiment (Fig. 2c). Indeed for electrode thicknesses above 4 nm, the coercive biases are stable and well-behaved as can be seen in the standard deviations of the data (Fig. 2d inset) but there is, in general, a small change in the film coercivity (defined as half the difference between coercive biases) (Fig. 2d).

As for the piezoresponse amplitude, we see similar traits to that observed for coercive biases. In Fig. 2e we see a drastic decrease in the magnitudes of the piezoresponses which would be consistent with the appearance of a ‘dot’ at the point of the tip-surface contact. For the 4 nm electrode (Fig. 2f) we again see erratic behavior however there is a semi-periodic nature (also visible to a lesser extent in the 11 nm case). The origin of this is a technical limitation of capturing only 20 hysteresis loops at once with a pause between resulting in a ‘burn-in’ upon the resumption of measurement. This could be an indication of a reversible change in the electrode structure or the accumulation of local charges which dissipate during the pause in measurement. As is the case with the coercive biases, stable piezoresponse behavior can be seen for electrodes > 4 nm (see Fig. 2g) however there is a general trend as summarized in Fig. 2h. For electrodes with thickness > 4 nm the total piezoresponse (average of the two piezoresponse magnitudes) only increases.

The trend of increased piezoresponse with switching indicates a change in the system with bias cycling. This effect could be described as a migration of oxygen vacancies or a change in the electrode properties due to local heating from the high current densities found in the vicinity of the tip apex [38].

In Fig. 3 we compare the case of tip switching on the film surface with that of the 11 nm-thick top electrode. We take loop no. 5 and 100 for comparison in both cases. The electrode case maintains the perfect rectangular loop structure while the film case shows a vast change in hysteresis as expected from Fig. 2a and e. Here we describe the differences in switching with respect to the measurement technique. In Fig. 3c the schematics depict the situation of switching in the $1 \times 1 \mu\text{m}^2$ capacitors. The polarization is switched through nucleation and forward growth of a reverse domain and associated 180° domain walls (Fig. 3c *i*). The domain walls then propagate radially in the ‘lateral expansion’ phase of domain growth (Fig. 3c *ii*). During this stage at some point the entire volume from which the

PFM signal is obtained *i.e.* signal generation volume [39] is switched and the piezoresponse value attains a maximum in the hysteresis loop. With continued growth the domain wall propagates to the outer edges of the electroded area completing the switching (Fig. 3c *iii*). We can tell from the abruptness of the switching that nucleation and domain wall growth beyond the signal generation volume (Fig. 3c *i* and *ii*) happens on a timescale <0.5 ms; this is the minimum time increment between acquired data points and outlines the time resolution of the measurement. With knowledge of the domain wall velocities as a function of electrode thickness [13], we can estimate the time required for full capacitor switching. For the slowest domain wall (4 nm electrode) we estimate full capacitor switching within 20 ms, that is, two voltage pulses/data points on the hysteresis loop. For all thicker electrodes we expect full capacitor switching to occur within one voltage pulse, *i.e.* <10 ms. Therefore the hysteresis loops here, *although acquired at a single point are indicative of/identical to the entire capacitor switching characteristics*. For switching to the original polarization direction a new nucleus is formed (Fig. 3c *iv*) and the same process occurs (stages *i-iii*).

For the tip-surface case the nucleation and lateral growth stage can clearly be inferred from the original shape of the hysteresis loop (Fig. 3b). The sharp change in piezoresponse indicates nucleation and rapid forward growth while the slowly varying section indicates lateral expansion within the signal generation volume. We assume the domain wall never moves beyond this limit as the piezoresponse does not reach saturation. The sharp change in piezoresponse on both positive and negative switching indicates that nucleation only occurs underneath the tip and not through backswitching of a pre-existing domain *i.e.* drawing the previously created wall towards the tip. In this scenario the new domain wall (Fig. 3d *iii*) moves towards the ‘old’ previous wall and at some point they will annihilate (Fig. 3d *iv*).

Having previously analysed the principal characteristics of the hysteresis loop, we now turn our attention to the shape of the loop. To this end we have normalised each switching loop to the

minimum and maximum piezoresponse at zero bias in order to overlay the loops on the same plot to better visualise the evolution with switching cycles (Fig. 3e). It is clear that in addition to the loop broadening the ‘wings’ of the loop are expanded meaning that the lateral expansion of the domain growth takes a relatively larger portion of time. Here we also see a separation of the nucleation and coercive biases. We see that the nucleation and forward growth phases become less significant in comparison to the slowly varying piezoresponse which we associate with the lateral expansion phase. This clear separation between these phases is not seen in the case for top electrodes. This again indicates that top electrodes of sufficient thickness allow for well-behaved and stable switching in the absence of significant electrochemistry that hampers switching with the tip alone.

3.2 Silicon oxide insulating layer

In order to provide a complementary but counterpoint case, we then looked at how the thickness of an insulating silicon oxide layer affected the switching characteristics (Fig. 4). It has been shown that that insulating layers strongly affect hysteresis [23][40]. From Fig. 4e we can see that upon increasing thickness the magnitudes of the coercive biases increases. Usually a ‘dead’ or ‘passive’ layer is used to describe similar effects [41] however studies of *intentionally* produced passive dielectric layers are not so common [22][23][26][40][42][43]. A simple, consistent explanation is a decrease in the effective field experienced by the ferroelectric film due to the voltage drop across the low permittivity silicon oxide layer. The main difference from the electrode case is that domain walls are not free to propagate (Fig. 4c,d). In fact the written domains are similar in size to those written with the tip only on the bare film surface (Fig. 4c,d insets). Therefore we can locally increase the magnitude of the coercive biases but limit the domain wall propagation. Also, the hysteresis loop shape reflects these changes (Fig. 4f). On the film we see the usual abrupt change in piezoresponse signalling nucleation and a slowly varying section associated with lateral expansion. For the switching with the silicon oxide layer we see a broadening in the width of the loop indicating its increased coercive biases and that the overall shape of the loop is much more rounded with an increased ‘tilt’ as could be expected from theory [44]. Finally we see that the piezoresponse decreases dramatically with increasing silicon

oxide layer thickness (Fig. 4g) indicating a similar damping of electromechanical oscillations to that seen in Fig. 1e.

4. Summary and Conclusions

In summary, we have shown that changing the thickness of EBID Pt top electrodes has some profound effects on the nucleation and switching characteristics of PZT thin films which we link to changes in work function. For electrode thicknesses below 10 nm the nucleation bias magnitudes more than double with respect to the tip-on-surface case. This might need to be taken into consideration when devising new nanoelectronic ferroelectric devices especially those involving EBID metals that allow control of domain wall positions. Future work could combine EBID metal electrodes with insulating silicon oxide layers so that the coercive biases can be tuned locally either with or without changing the local internal field.

Acknowledgements

The Swiss National Science Foundation (grant no. 200020_153177) is acknowledged for financial support. The research leading to these results received funding also from the European Research Council under the EU 7th Framework Programme (FP7/2007–2013)/ERC grant agreement no. 268058 Mobile-W. The authors acknowledge enlightening discussions with Dr. T. Sluka and Dr. A. Crassous.

References

- [1] E. A. Little, Dynamic Behavior of Domain Walls in Barium Titanate, *Phys. Rev.* 98 (1955) 978.
- [2] S. M. Yang, J.-G. Yoon, T. W. Noh, Nanoscale Studies of Defect-Mediated Polarization Switching Dynamics in Ferroelectric Thin Film Capacitors, *Curr. Appl. Phys.* 11 (2011) 1111.
- [3] W. J. Merz, Domain Formation and Domain Wall Motions in Ferroelectric BaTiO₃ Single Crystals, *Phys. Rev.* 95 (1954) 690.

- [4] J. R. Whyte, R. G. P. McQuaid, P. Sharma, C. Canalias, J. F. Scott, A. Gruverman, J. M. Gregg, Ferroelectric Domain Wall Injection, *Adv. Mater.* 26 (2014) 293.
- [5] J. R. Whyte, R. G. P. McQuaid, C. M. Ashcroft, J. F. Einsle, C. Canalias, A. Gruverman, J. M. Gregg, Sequential injection of domain walls into ferroelectrics at different bias voltages: Paving the way for “domain wall memristors”, *J. Appl. Phys.* 116 (2014) 066813.
- [6] J. R. Whyte, J. M. Gregg, A diode for ferroelectric domain-wall motion, *Nat Commun.* 6 (2015) 7361.
- [7] L. J. McGilly, P. Yudin, L. Feigl, A. K. Tagantsev, N. Setter, Controlling domain wall motion in ferroelectric thin films, *Nature Nanotech.* 10 (2015) 145.
- [8] L. J. McGilly, L. Feigl, X. Dai, N. Setter, Polarization Switching and Domain Wall Motion in Circular and Ring Capacitor Structures in PZT Thin Films, *Ferroelectrics* 480 (2015) 58.
- [9] L. J. McGilly, C. S. Sandu, L. Feigl, D. Damjanovic, N. Setter, Nanoscale Defect Engineering and the Resulting Effects on Domain Wall Dynamics in Ferroelectric Thin Films, *Adv. Func. Mater.* doi: 10.1002/adfm.201605196
- [10] J. J. L. Mulders, Purity and resistivity improvements for electron-beam-induced deposition of Pt, *Appl. Phys. A* 117 (2014) 1697.
- [11] A. Botman, J. J. L. Mulders, C. W. Hagen, Creating pure nanostructures from electron-beam-induced deposition using purification techniques: a technology perspective, *Nanotechnology* 20 (2009) 372001.
- [12] W. F. van Dorp, C. W. Hagen, The influence of beam defocus on volume growth rates for electron beam induced platinum deposition, *Nanotechnology* 19 (2008) 485302.
- [13] L. J. McGilly, L. Feigl, T. Sluka, P. Yudin, A. K. Tagantsev, N. Setter, Velocity Control of 180° Domain Walls in Ferroelectric Thin Films by Electrode Modification, *Nano Lett.* 16 (2016) 68.
- [14] A. Perentes, P. Hoffmann, Focused Electron Beam Induced Deposition of Si-Based Materials From SiO_xC_y to Stoichiometric SiO_2 : Chemical Compositions, Chemical-Etch Rates, and Deep Ultraviolet Optical Transmissions, *Chem. Vap. Deposition* 13 (2007) 176.
- [15] B. J. Rodriguez, C. Callahan, S. V. Kalinin, R. Proksch, Dual-frequency resonance-tracking atomic force microscopy, *Nanotechnology* 18 (2007) 475504.
- [16] S. Jesse, A. P. Baddorf, S. V. Kalinin, Switching spectroscopy piezoresponse force microscopy of ferroelectric materials, *Appl. Phys. Lett.* 88 (2006) 062908.
- [17] L. Jin, F. Li, S. Zhang, Decoding the Fingerprint of Ferroelectric Loops: Comprehension of the Material Properties and Structures, *J. Am. Ceram. Soc.* 97 (2014) 1.
- [18] L. Wang, Y. Dai, L. Yang, J. Xu, L. Zou, B. Tian, D. Huang, Effect of top electrode thickness on the piezoresponse of polycrystalline ferroelectric capacitors, *J. Phys. D: Appl. Phys.* 45 (2012) 505302.
- [19] J. Lee, C. H. Choi, B. H. Park, T. W. Noh, J. K. Lee, Built-in voltages and asymmetric polarization switching in $\text{Pb}(\text{Zr,Ti})\text{O}_3$ thin film capacitors, *Appl. Phys. Lett.* 72 (1998) 3380.
- [20] K.-W. Lee, Y.-I. Kim, W.-J. Lee, Physical Modeling of the Effect of the Asymmetric Electrode Configuration on the Hysteresis Curves of Ferroelectric Film Capacitors, *Ferroelectrics*, 271 (2002) 179.

- [21] A. K. Tagantsev, G. Gerra, Interface-induced phenomena in polarization response of ferroelectric thin films, *J. Appl. Phys.* 100 (2006) 051607.
- [22] G. Liu, J. Chen, C. Lichtensteiger, J.-M. Triscone, P. Aguado-Puente, J. Junquera, N. Valanoor, Positive Effect of an Internal Depolarization Field in Ultrathin Epitaxial Ferroelectric Films, *Adv. Electron. Mater.* 2 (2016) 1500288.
- [23] C. Lichtensteiger, C. Weymann, S. Fernandez-Pena, P. Paruch, J.-M. Triscone, Built-in voltage in thin ferroelectric PbTiO₃ films: the effect of electrostatic boundary conditions, *New J. Phys.* 18 (2016) 043030.
- [24] V. P. Afanasjev, A. A. Petrov, I. P. Pronin, E. A. Tarakanov, E. J. Kaptelov, J. Graul, Polarization and self-polarization in thin PbZr_{1-x}Ti_xO₃ (PZT) films, *J. Phys.: Condens. Matter* 13 (2001) 8755.
- [25] L. Feigl, P.-E. Janolin, T. Yamada, M. Iwanowska, C. S. Sandu, N. Setter, Post-deposition control of ferroelastic stripe domains and internal electric field by thermal treatment, *Appl. Phys. Lett.* 106 (2015) 032902.
- [26] C. Lichtensteiger, S. Fernandez-Pena, C. Weymann, P. Zubko, and J.-M. Triscone, Tuning of the Depolarization Field and Nanodomain Structure in Ferroelectric Thin Films, *Nano Lett.* 14 (2014) 4205.
- [27] C. Marliere, Quantum size effect detected by work function measurements during indium deposition on polycrystalline, texturized gold substrate, *Vacuum* 41 (1990) 1192.
- [28] C. M. Wei, M. Y. Chou, Theory of quantum size effects in thin Pb(111) films, *Phys. Rev. B* 66 (2002) 233408.
- [29] J. J. Paggel, C. M. Wei, M. Y. Chou, D.-A. Luh, T. Miller, T.-C. Chiang, Atomic-layer-resolved quantum oscillations in the work function: Theory and experiment for Ag/Fe(100), *Phys. Rev. B* 66 (2002) 233403.
- [30] R. M. Langford, T.-X. Wang, D. Ozkaya, Reducing the resistivity of electron and ion beam assisted deposited Pt, *Microelectron. Eng.* 84 (2007) 784.
- [31] A. Ilie, A. Hart, A. J. Flewitt, J. Robertson, Effect of work function and surface microstructure on field emission of tetrahedral amorphous carbon, W. I. Milne, *J. Appl. Phys.* 88 (2000) 6002.
- [32] R. D. Forrest, A. P. Burden, S. R. P. Silva, L. K. Cheah, X. Shi, A study of electron field emission as a function of film thickness from amorphous carbon films, *Appl. Phys. Lett.* 73 (1998) 3784.
- [33] H. B. Michaelson, The work function of the elements and its periodicity, *J. Appl. Phys.* 48 (1977) 4729.
- [34] A. J. Hartmann, M. Neilson, R. N. Lamb, K. Watanabe, J. F. Scott, Ruthenium oxide and strontium ruthenate electrodes for ferroelectric thin-films capacitors, *Appl. Phys. A* 70 (2000) 239.
- [35] L. Pintilie, I. Vrejoiu, D. Hesse, M. Alexe, The influence of the top-contact metal on the ferroelectric properties of epitaxial ferroelectric Pb(Zr_{0.2}Ti_{0.8})O₃ thin films, *J. Appl. Phys.* 104 (2008) 114101.
- [36] I. Pintilie, C. M. Teodorescu, C. Ghica, C. Chirila, A. G. Boni, L. Hrib, I. Pasuk, R. Negrea, N. Apostol, L. Pintilie, Polarization-Control of the Potential Barrier at the Electrode Interfaces in Epitaxial Ferroelectric Thin Films, *ACS Appl. Mater. Interfaces* 6 (2014) 2929.

- [37] R. Nigon, N. Chidambaram, T. M. Raeder, P. Muralt, Influence of asymmetric electrodes on the switching of PZT thin films, 2015 Joint IEEE International Symposium on the Applications of Ferroelectric (ISAF), International Symposium on Integrated Functionalities (ISIF), and Piezoelectric Force Microscopy Workshop (PFM) (2015) 193 DOI: 10.1109/ISAF.2015.7172703
- [38] S. V. Kalinin, S. Jesse, A. Tselev, A. P. Baddorf, N. Balke, The Role of Electrochemical Phenomena in Scanning Probe Microscopy of Ferroelectric Thin Films, *ACS Nano*. 7 (2011) 5683.
- [39] S. V. Kalinin, E. Karapetian, M. Kachanov, Nanoelectromechanics of piezoresponse force microscopy, *Phys. Rev. B* 70 (2004) 184101.
- [40] M. McMillen, A. M. Douglas, T. M. Correia, P. M. Weaver, M. G. Cain, J. M. Gregg, Increasing recoverable energy storage in electroceramic capacitors using “dead-layer” engineering, *Appl. Phys. Lett.* 101 (2012) 242909.
- [41] A. K. Tagantsev, I. A. Stolichnov, Injection-controlled size effect on switching of ferroelectric thin films, *Appl. Phys. Lett.* 74 (1999) 1326.
- [42] H. Lu, X. Liu, J. D. Burton, C.-W. Bark, Y. Wang, Y. Zhang, D. J. Kim, A. Stamm, P. Lukashev, D. A. Felker, C. M. Folkman, P. Gao, M. S. Rzechowski, X. Q. Pan, C.-B. Eom, E. Y. Tsybal, A. Gruverman, Enhancement of Ferroelectric Polarization Stability by Interface Engineering, *Adv. Mater.* 24 (2012) 1209.
- [43] A. Ghosh, G. Koster, G. Rijnders, Tunable and temporally stable ferroelectric imprint through polarization coupling, *APL Mater.* 4 (2016) 066103.
- [44] A. K. Tagantsev, M. Landivar, E. Colla, N. Setter, Identification of passive layer in ferroelectric thin films from their switching parameters, *J. Appl. Phys.* 78 (1995) 2623.

Fig. 1. (a) A schematic representation of the structure under investigation with a 3D topography image showing the EBID Pt electrodes of different thicknesses deposited on a PZT(10/90) thin film. PFM amplitude (b) and phase (c) images of the bare film surface in the as-grown state shows uniform polarization out-of-plane, oriented away from the substrate. Examples of hysteresis loops obtained on 3 different electrode thicknesses and on the bare film surface (d). Loop no.5 in the 100-loop sequence is shown. The piezoresponse (at zero dc bias) as a function of electrode thickness (e) [blue (orange): positive (negative) state piezoresponse]. Zero electrode thickness is taken to mean the tip on bare film surface (square points). The coercive biases as a function of electrode thickness and imprint (grey point and lines) (f). Comparison of different data sets shows this coercive behavior to be broadly consistent across several experiments (g). The solid black lines are a 3-point moving average of the respective data sets and the grey line is the associated imprint.

Fig. 2. Evolution with hysteresis loop cycling. Coercive biases (positive: blue, negative: orange) and piezoresponse for the tip on film surface (a) and (e), electrode of thickness 4 nm (b) and (f) and 11 nm (c) and (g). Percentage change in coercivity (d) and total piezoresponse (h) from start to end of hysteresis loop acquisition for the range of electrode thicknesses (tip-on-film: square points). The inset to (d) shows the standard deviation, σ , of the coercive biases.

Fig. 3. Comparison of hysteresis loops no.5 and no.100 for 11 nm-thick electrode (a) and for tip on film surface (b). Schematic description of proposed switching mechanisms in electroded (c) versus tip case (d) with side view: top and plan view: bottom. The tip is shown in grey, EBID Pt electrodes in yellow, upwards polarization (red arrow) in the PZT thin film is blue and downwards is green. The SRO bottom electrode is orange. The white dotted circle outlines the signal generation volume and orange outline in (c) plan view shows the electrode outline. (e) Evolution of loop shape for the tip-surface case. Positive and negative piezoresponse values at zero dc bias are normalised to +1 and -1 respectively and the line colour gives the loop number as shown in the legend.

Fig. 4. (a) Schematic of setup with insulating layer of silicon oxide (purple). Topography image of a $2 \times 2 \mu\text{m}^2$ EBID silicon oxide of thickness 4 nm (b) and PFM amplitude (c) and phase (d) of a switched domain similar in size to that obtained outside the insulating layer on the bare-film surface (insets). (e) Coercive biases averaged from 10 hysteresis loops (positive: blue, negative: orange and imprint: grey, square points: tip-on-film) as a function of the thickness of the silicon oxide. Error bars are standard deviations. Example hysteresis loops on the film versus that on a silicon oxide layer of thickness 7.8 nm (f). Note that the unusual drop in piezoresponse observable in the ‘film’ loop is assumed to be due

to leakage through the film at the high applied bias of ~ 10 V. Change in piezoresponse as a function of insulating layer thickness (square point: tip-on-film) (g).

ACCEPTED MANUSCRIPT

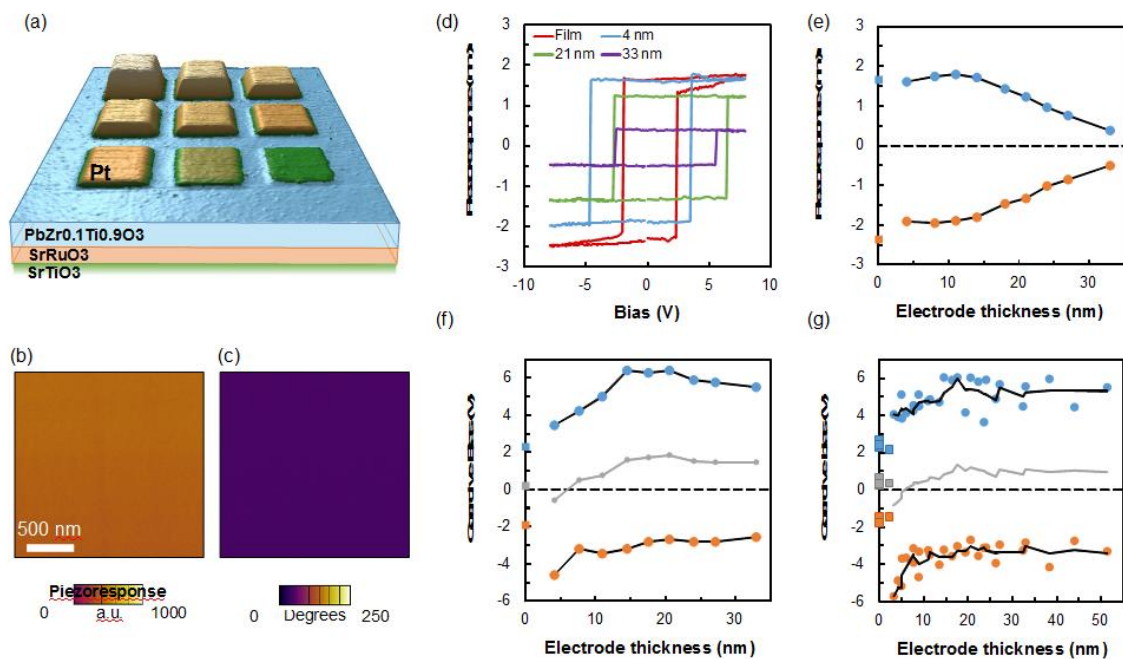


Figure 1

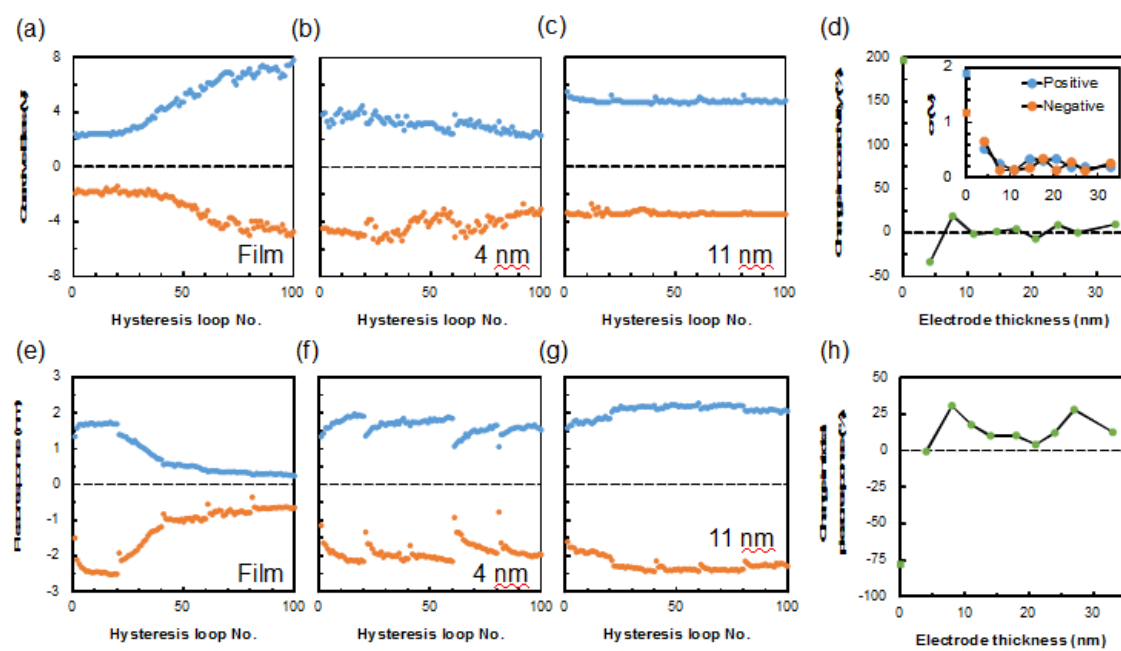


Figure 2

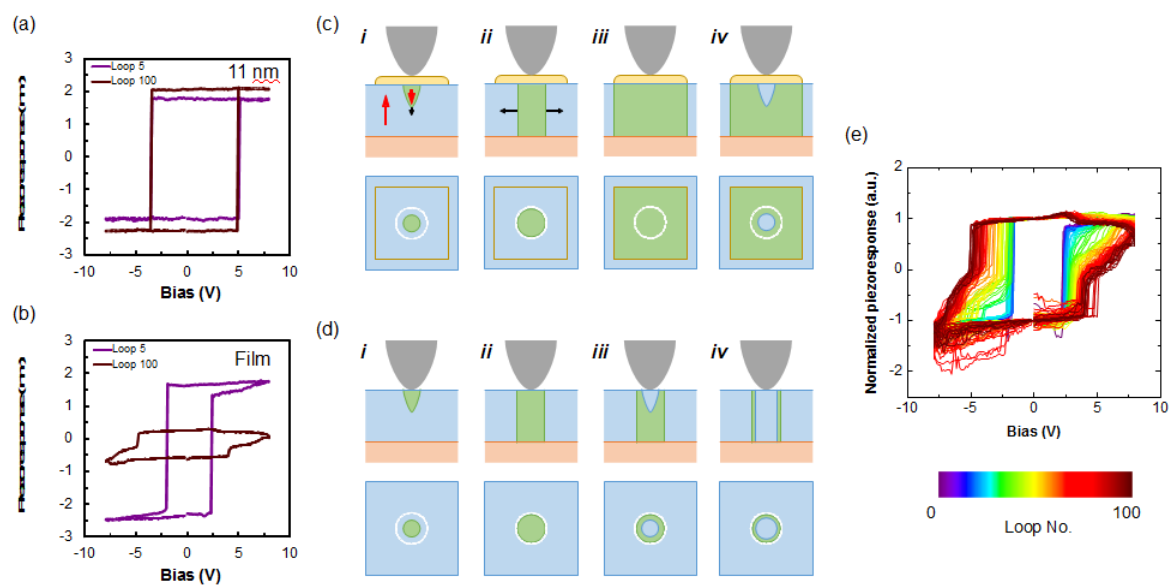


Figure 3

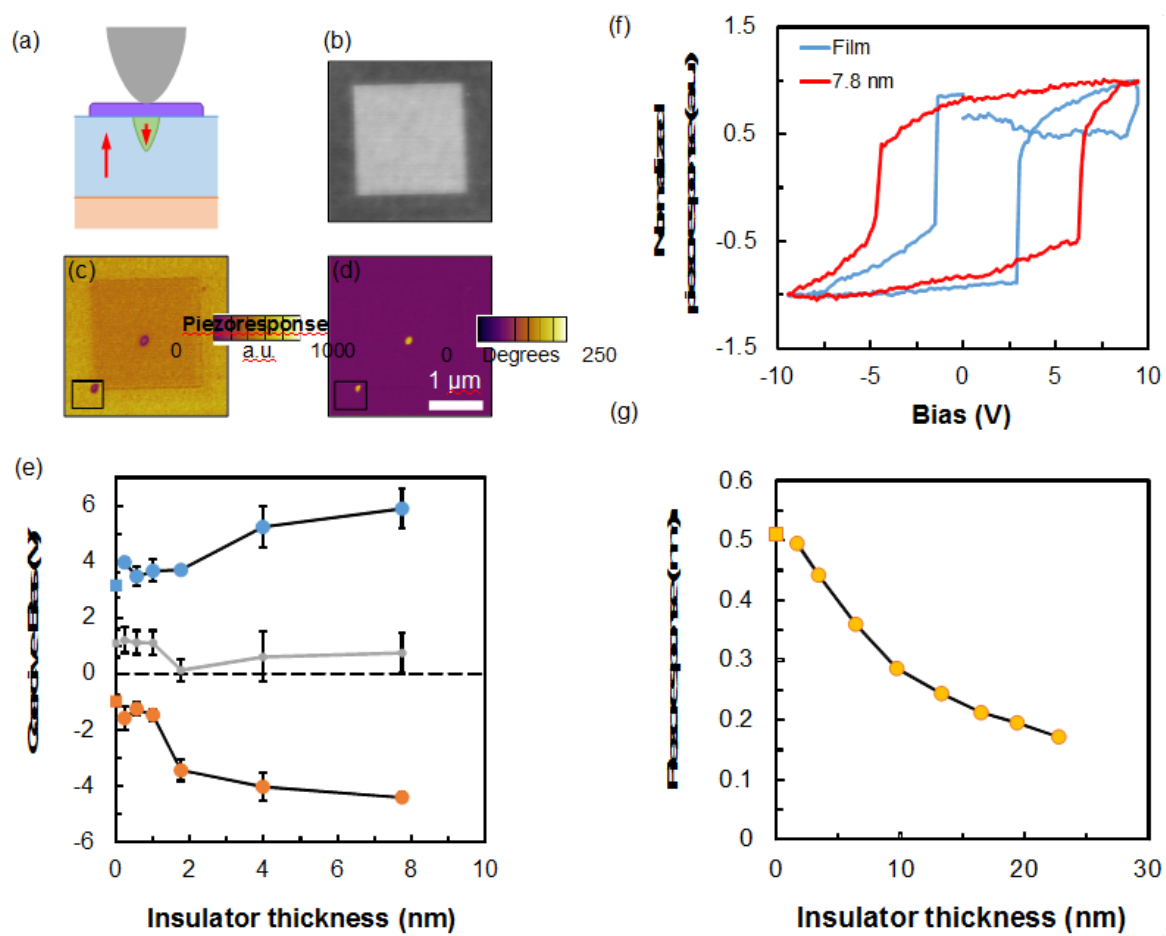


Figure 4

Highlights

- Change in sign of ferroelectric imprint due to electrode thickness variations
- Evolution of coercive biases and piezoresponse with hysteresis loop cycling
- Comparison of switching with electrode versus piezoresponse force microscopy tip
- Deposition and study of the effect of insulating silicon oxide layer on hysteresis

ACCEPTED MANUSCRIPT